# THE SUMMERTIME ARCTIC ATMOSPHERE

## Meteorological Measurements during the Arctic Ocean Experiment 2001

BY MICHAEL TJERNSTRÖM, CAROLINE LECK, P. OLA G. PERSSON, MICHAEL L. JENSEN, STEVEN P. ONCLEY, AND ADMIR TARGINO

A summer expedition with the Swedish icebreaker *Oden* found a moist, cloudy, but well-mixed Arctic boundary layer, with a persistent capping inversion, many shallow mesoscale fronts, and features generally unique to polar conditions.

In recent years, scientists and scientific organizations have increasingly stressed the significance of the Arctic in the global climate system. The past decade has seen changes in near-surface air temperature, ice extent, and upper-ocean stratification (Houghton et al. 2001), suggesting that anthropogenic climate change has begun to affect the Arctic. Serreze et al. (2000) discuss significant temperature increases over the northern Eurasian and American landmasses of > 0.5°C per decade, while Rigor et al. (2000) find trends in winter temperatures of ~ +1°C per decade on the Eurasian side of the Arctic. Generally, these trends agree with the trends in the Arctic Oscillation (Thompson and Wallace 1998). Morison et al. (2000) discuss the inflow of warm and saline Atlantic water that recently has penetrated deeper into the Arctic, altering upper-ocean stability. Chapman and Walsh (1993) show a downward long-term trend in sea ice extent for 1961–90. Parkinson et al. (1999) show that Arctic sea ice extent has been decreasing by ~ 3% per decade, using microwave data through 1996, while Comiso (2002) shows that the perennial sea ice extent is decreasing by > 9% per decade.

The Arctic is often assumed to have a large climate sensitivity, and anthropogenic climate change is projected to be the largest in the Arctic (e.g., Houghton et al. 2001). Arctic warming is ~ 2.5 times the global average in the Coupled Model Intercomparison Project (CMIP; Meehl et al. 2000) simulations (Räisänen 2001). However, the global models used for these projections have problems reproducing even the

**AFFILIATIONS:** TJERNSTRÖM, LECK, AND TARGINO—Stockholm University, Stockholm, Sweden; PERSSON—National Oceanic and Atmospheric Administration/Environmental Technology Laboratory, and Cooperative Institute for Research in Environmental Studies, Boulder, Colorado; JENSEN—Cooperative Institute for Research in Environmental Studies, Boulder, Colorado; ONCLEY—National Center for Atmospheric Research, Boulder, Colorado
A supplement to this article is available online (DOI:10.1175/BAMS-84-9-Tjernstrom)
**CORRESPONDING AUTHOR:** Dr. Michael Tjernström, Arrhenius Laboratory, Department of Meteorology, Stockholm University, Stockholm S-106 91, Sweden
E-mail: michaelt@misu.su.se
DOI:10.1175/BAMS-85-9-1305

In final form 12 April 2004

current Arctic climate. They are generally too warm and have systematic biases in the surface pressure fields, with surface radiative fluxes varying widely between models (Walsh et al. 2002). Consequently, the intermodel spread in CMIP climate-warming scenarios is larger in the Arctic than elsewhere (Räisänen 2001). The observed recent warming also appears to have occurred mostly over the northern Eurasian continent, rather than over the central Arctic, as had been suggested by many climate models (Serreze et al. 2000).

The difficulties in simulating the Arctic climate relate directly to an insufficient understanding of several strong feedback processes. The large climate sensitivity in models is due largely to the strongly positive ice–albedo feedback: warming reduces the ice/snow cover, thereby reducing the surface albedo, thus, enhancing the warming. How climate models handle sea ice and snow, and the energy exchange at the surface is, therefore, critical. Battisti et al. (1997) showed that a lack of physical detail in describing ice processes inhibits a realistic representation of natural variability in the Arctic climate. It also causes significant errors in global weather forecast models (Beesley et al. 2000).

The ice/snow cover also has a pronounced effect on the turbulent surface fluxes. During winter, snow-covered ice insulates the atmosphere from the high heat capacity of the ocean. Combined with longwave radiative cooling and the absence of solar forcing during the Arctic winter, this gives rise to persistent stable stratification in the Arctic boundary layer (ABL) about 75% of the time (Persson et al. 2002). Turbulence in very stable conditions is poorly understood (Mahrt 1998; Grachev et al. 2004). During summer, melting ice and snow regulates the low-level temperature; additional energy input enhances melting rather than heating the surface, while energy loss results in freezing, rather than a cooling. When this unique surface interacts with local boundary layer processes, it gives rise to a vertical structure found only in the Arctic.

Long periods of stable ABL conditions are interspersed with shorter periods with near-neutral conditions. This is forced by longwave radiation (Persson et al. 2002) and directly related to boundary layer clouds, which are a known problem in models. Liquid water droplets are present in a sizeable fraction even at very low temperatures (Beesley et al. 2000; Intrieri et al. 2002b), and unusual vertical structures with layering and decoupling from the surface are described by Curry et al. (2000). Clouds play an important role for the surface radiative fluxes, determining the net longwave radiation and regulating incoming solar radiation in summer. Over the Arctic pack ice, in contrast to midlatitude oceans, clouds often lead to surface warming (Intrieri et al. 2002a). Curry (1986) discusses the connection of cloud effects to aerosol particles and cloud microphysics. During summer, the influence of anthropogenic aerosol sources is limited in the Arctic due to the typical large-scale circulations, and by efficient scavenging (Leck et al. 1996). The lack of aerosol particles, vital to the formation of cloud condensation nuclei (CCN), regulates the radiative characteristics of the clouds, providing possible complications to the ice–albedo feedback. If increased open water from enhanced melting also results in an increase in the concentration of aerosols from local biogenic sources, this may increase the reflectivity and change the lifetime of Arctic stratus clouds. This would constitute a negative feedback to climate change.

Many of these factors are specific to the Arctic. The ice cover is also a reason for a relative lack of in situ observations, while producing a difficult and hostile environment for observational studies. Moreover, because the ice drifts, fixed permanent sites for long-term measurements cannot be established. Consequently, the ensemble of observations forming the empirical basis for the development of reliable parameterizations may be inadequate. This may be one reason for the difficulties in modeling the Arctic climate, and the only realistic way to rectify this is to obtain detailed observations of climate-related processes in the Arctic. Detailed observations of the Arctic surface layer and the energy balance at the surface, as well as vertical troposphere structure, are available from the Surface Heat Budget of the Arctic Ocean (SHEBA; Uttal et al. 2002; Perovich et al. 1999) and, during a shorter period, the First International Satellite Cloud Climatology Project (ISCCP) Regional Experiment (FIRE) Arctic Clouds Experiment (Curry et al. 2000) complemented SHEBA with detailed airborne measurements. Recently, observations made on Russian drifting North Pole stations were also made available (e.g., Kahl et al. 1999).

The atmospheric program during the summer of 2001 [Arctic Ocean Experiment (AOE) 2001; Leck et al. 2004] on the Swedish icebreaker *Oden* was the third in a series of similar expeditions. The previous two expeditions in 1991 [International AOE (IAOE)-91; Leck et al. 1996] and 1996 (AOE-96; Leck et al. 2001a) were focused on studying atmospheric chemistry and aerosol chemistry/physics. We designed AOE-2001 to improve upon the previous observational work by adding an enhanced meteorological

component, a better vertical profiling capability for examining atmospheric chemistry and aerosols, and a marine biology component to investigate processes in open leads and ice. We attempted to characterize a column from a few hundred meters into the ocean, through the ice–ocean interface, up to a few kilometers into the atmosphere. AOE-2001 was an interdisciplinary experiment with three subprograms: marine biology, atmospheric chemistry and aerosol chemistry/physics, and meteorology (more information available online at www.lu.se/eriksw/AOE-2001.html). Although this experiment was significantly shorter than SHEBA, AOE-2001 had a stronger focus on boundary layer structure. In addition, it was carried out in the Atlantic sector of the Arctic, which has received comparatively less attention—at least for the atmosphere—and was significantly farther north. Moreover, SHEBA almost entirely lacked the atmospheric chemistry and aerosol components present in AOE-2001.

The results from previous expeditions on *Oden* showed that in addition to the strong and well-defined biogenic source of dimethylsulfides (DMS; an important aerosol precursor; Leck and Persson 1996) in the marginal ice zone (MIZ), a previously unknown local source of aerosols in the pack ice seems to be present. It was speculated that this local source was also biogenic, located in open leads (Leck and Bigg 1999; Bigg and Leck 2001; Leck et al. 2001b). Also, temporal variability of concentrations of aerosol and gases (e.g., DMS and $NH_3$) were unexpectedly large, with time scales from minutes to hours. Order-of-magnitude changes within a day were not uncommon (Bigg et al. 1996, 2001). AOE-2001 was conceived to better address these issues. This paper presents the AOE-2001 field program, focusing on the meteorological measurements. There are three main purposes for the meteorology subprogram:

1) to study and determine likely causes for the previously observed temporal variability in gases and aerosols;
2) to study boundary layer mixing processes of importance for the energy balance at the surface, and for bringing newly formed particles into the ABL from the surface or bringing long-range-transported aerosol precursors down from the free troposphere; and
3) to collect boundary layer meteorology data that will enhance the understanding of the summertime ABL dynamics and, thus, help to improve model formulations.

**THE EXPEDITION.** *Oden* (Fig. 1) is a diesel-powered, 108-m-long, 24,500-hp icebreaker, built in Sweden in 1988 to assist in commercial shipping. *Oden* is particularly effective in the Arctic, capable of breaking 2-m-thick ice continuously at a speed of 3 kt, and was the first non-nuclear-powered icebreaker to reach the North Pole in July 1991. During the present expedition, the atmospheric program shared *Oden* with other scientific programs: biogeochemistry, oceanography, and seismology. The expedition segments had different scientific priorities that determined the cruise plan and onboard activity. Parts of the atmospheric measurements were conducted continuously; a 3-week ice drift (2–21 August 2001) was the main target period for the atmospheric program.

The track of the expedition is shown in Fig. 2. The expedition departed Gothenburg, Sweden, on 29 June 2001, and the first research station was set up southeast of Svalbard on 5 July; two stations were established in this area. The expedition continued with two more MIZ stations (9–10 and 11–12 July) and after establishing one more southerly research station in open water northwest of Svalbard (15–16 July), *Oden*


**FIG. 1. Picture of the icebreaker *Oden* at the ice camp. The blue containers carried research equipment or housed various laboratories. The tethered balloon is visible at the stern.**

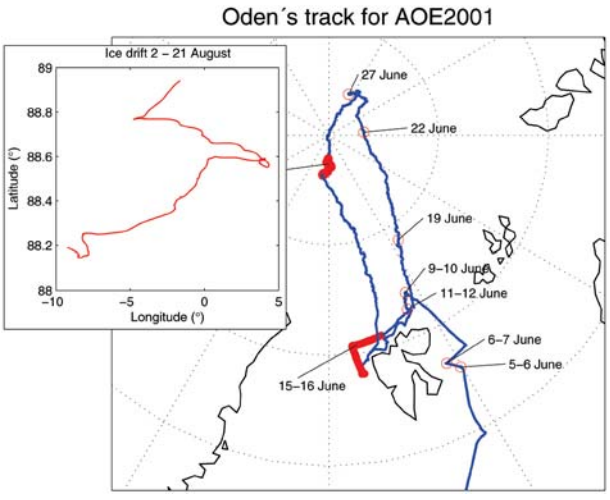


**FIG. 2. Plot of *Oden's* track during AOE-2001, giving dates and locations for the atmospheric research stations. The insert shows the track while drifting with a large ice floe for the main 3-week atmospheric campaign.**

headed into the pack ice on 17 July and traversed the Gakkel ridge and Amundsen basin to the Lomonosov ridge. Three more atmospheric research stations were established (on 19, 22, and 27 July) before reaching the North Pole on 31 July. During all of the shorter station periods, many of the biology and atmospheric chemistry/aerosol subprograms were active; however, the meteorology subprogram was mostly limited to remote sensing instruments on board, rawinsoundings, and the *Oden* weather station, due to insufficient time to deploy the appropriate instruments on the ice, although the tethered sounding system and an Integrated Surface Flux Facility (ISFF) station was temporarily deployed a few times.

On 2 August *Oden* was moored to a relatively flat ~ 1.5 km × 3 km ice floe at ~ 89°N, 1°W (Fig. 3). Ice thickness varied from ~ 1.5 to greater than 8 m, with the latter at the site of the ice camp, presumably due to subsurface ridging. The ice surface was covered with melt ponds of various sizes (see Fig. 3). Some ponds eventually froze and became snow covered. Although August is at the end of the melt season, the ice was stable for the duration of the experiment and the ice drift continued with *Oden* attached to the same ice floe until 21 August. During this 3-week period, we drifted about 150 km in a generally southwesterly direction (see insert to Fig. 2).

**METEOROLOGICAL MEASUREMENTS.** The objectives of the meteorological measurements called for both a continuous monitoring of the vertical structure of the lower troposphere at a high temporal resolution and detailed ABL process studies. Although vertical structure was a main focus, we also wanted information on the horizontal structure and propagation of mesoscale systems. The measurement systems that were deployed reflected all these needs.

A suite of remote sensing instruments was deployed on *Oden,* some later on the ice, to provide a continuous record of vertical profiles of wind speed and direction, temperature, and clouds through the lower troposphere. Atmospheric moisture profiles were provided by the regularly released rawinsoundings. Detailed studies of ABL turbulence and mixing require an undisturbed environment. *Oden* affects measurements by disturbing airflow and from the noise generated by its fans and hydraulics; the ice drift was devised to alleviate these problems. Neighboring ice floes were also utilized for some measurements.

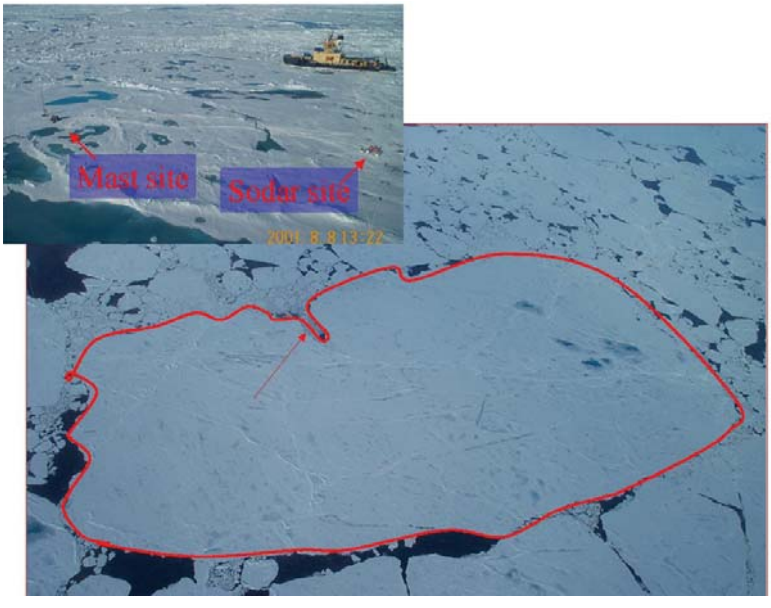


**FIG. 3. Aerial photograph of the ice floe used for the 3-week main atmospheric campaign taken from the helicopter (15 Aug). The harbor (indicated by red arrow) set up by *Oden* to be able to shift mooring positions to face upwind is visible in the upper edge of the ice floe. Most of the atmospheric program was carried out on the top-left quadrant of the ice floe. The insert photograph shows the surface conditions near the mast and the sodar/tether sites on 8 Aug. Note the amount of melt ponds early during the ice drift.**

A complete description of instrumentation can be found in an online supplement (Tjernström et al. 2004), so only a summary is provided here as follows:

- Standard measurements: A weather station on *Oden*'s top deck, ~ 30 m above the ocean surface, provided atmospheric variables and navigational information continuously throughout the expedition. Rawinsoundes were released from *Oden*'s helipad every 6 h during the ice drift and all shorter research stations.
- Remote sensing: A 915-MHz wind profiler, a scanning 5-mm radiometer for temperature profiles, and an S-band cloud and precipitation radar were deployed on board. Two sodar systems were deployed on the ice.
- Tethered soundings: The Cooperative Institute for Research in Environmental Sciences (CIRES) Tethered Lifting System (TLS) was operated on the ice. Three payloads, for basic meteorology, 3D turbulence, and aerosols, were flown in various combinations.
- The main mast: An 18-m meteorological telescoping mast about 300 m from *Oden* was equipped with wind and temperature profile and turbulence instruments. The measurements also included wind direction, absolute temperature, relative humidity, and a temperature profile into the ice, as well as radiation and atmospheric pressure at the surface.
- An array of microbarographs, for the detection of gravity waves, was operated at the ice camp with three sensors in a roughly equilateral triangular pattern ~ 200 m on each side, with a reference sensor in the center.
- Two ISFF stations were deployed on nearby ice floes ~ 8 km away from *Oden* to assess horizontal homogeneity. These stations, forming a roughly equilateral triangle with the main meteorological mast, made both turbulence and standard meteorological measurements.

**GENERAL ATMOSPHERIC CONDITIONS.** Time[1]–height cross sections of some atmospheric variables from the ice drift provide a useful starting point for a discussion of the vertical structure of the summer of 2001 Arctic atmosphere. Figure 4a shows quite a variable thermal structure in the free troposphere. There were several periods with very warm air aloft, and the highest temperature during the ice drift occurred on 11 August, when the temperature around 1 km reached 8°C. Other such periods with very warm air aloft occurred on 5–6 and 16–17 August. Such periods of warm air appear to be associated with advection of air from the open oceans south of the ice boundary and were associated with very strong vertical gradients in potential temperature,[2] $\Theta$, (see Fig. 4b).

Relative humidity aloft was also quite variable (Fig. 4c). During periods with synoptic-scale weather systems, such as during the first few days of the ice drift and around 11 and 16 August, the entire column had a high relative humidity. For other periods, low relative humidity (<40%) was found all of the way down to the ABL top (indicated by the thick, solid line), for example, around 10 August. The periods with the warmest air aloft were also often associated with an increase in specific humidity with height (Fig. 4d), sometimes even when relative humidity decreased.

The boundary layer remained relatively shallow and appeared to be well mixed (Fig. 4b) and capped by an inversion. The temperature within the ABL was relatively constant, in contrast to the free troposphere, and relative humidity remained high. Conditions in the ABL, thus, varied far less than in the free troposphere. From these plots, it would seem natural to assume that free-troposphere conditions were mostly governed by synoptic-scale variability and advection from the south, while ABL conditions were governed more by local mixing and surface properties in relative isolation from what happened aloft. In the following sections, we will examine these various regimes in more detail, starting aloft in the free troposphere and moving down into the ABL through the inversion.

**THE FREE TROPOSPHERE.** AOE-2001 was characterized by high synoptic-scale activity. Figure 5 shows the mean and anomaly fields of mean sea level pressure for July and August 2001 from the National Centers for Environmental Prediction (NCEP)–National Center for Atmospheric Research (NCAR) reanalysis project (Kalnay et al. 1996). The average sea

[1] During the whole experiment UTC was consistently used for measurement of time. For the ice drift, which is the focus in this paper, the longitude never deviated much from the Greenwhich meridian. Consequently, UTC and local time are roughly the same.

[2] Here, $\Theta = T(p/1000)^{\frac{R_d}{c_p}}$, where $T$ is the temperature, $p$ is the pressure, and $R_d$ and $c_p$ are the gas constant and heat capacity of dry air, respectively.

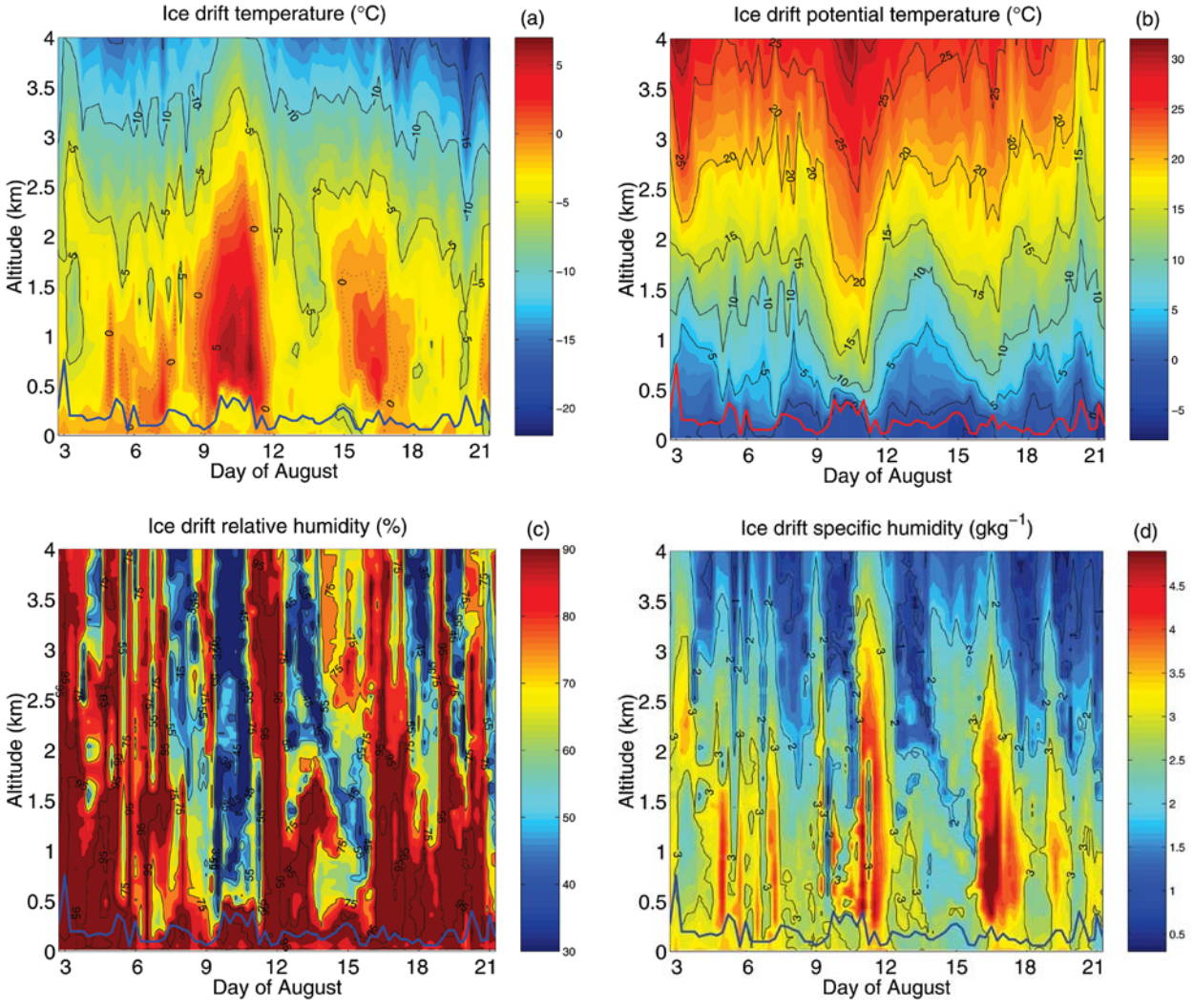


**Fig. 4. Rawinsonde time–height cross sections of the lower troposphere (up to 4 km) showing (a) temperature and (b) potential temperature (°C), (c) relative humidity with respect to water (%), and (d) specific humidity (g kg$^{-1}$) for the entire ice drift. The thick, solid lines (blue or red) show the top of the boundary layer.**

level pressure (Fig. 5a) shows the northern edge of the subtropical high pressure cells over the Atlantic and the Pacific Oceans with low-pressure areas over the Arctic, North Atlantic, and northern Asian continent. The pressure anomaly (Fig. 5b) shows stronger-than-average subtropical high pressure cells and lower-than-average pressure over the Arctic, in a pattern from the North Atlantic, along the Norwegian coast, continuing north of the Eurasian continent to Alaska. July contributed more to this pattern than August. A series of low pressure systems followed this path, and *Oden*'s track into the pack ice roughly followed the northern edge of this anomaly. There is a small region of higher-than-average pressure over the Greenland Sea and the ice drift moved roughly across the gradient north of this anomaly. Thus, AOE-2001 locations were often under the influence of synoptic cyclones. More quiescent periods of "high pressure weather" were also experienced, mostly toward the end of the experiment. It is likely that the Atlantic sector is more affected by synoptic-scale weather systems than the Beaufort/Chukchi Sea area, where SHEBA was situated, due to its location downstream from the North Atlantic storm track, although significant summertime synoptic activity was sometimes observed also during SHEBA (Persson et al. 2003).

Figure 6 shows a time–height cross section of the wind speed from rawinsoundings during the ice drift. High winds occur mostly during the first week, associated with synoptic-scale weather systems. Two shorter high-wind episodes are found on 11 and 16 August, also associated with synoptic-scale weather. Figure 7 shows

examples of the echo intensity (in $dBZ_e$) from the cloud and precipitation radar during the ice drift. In the first 4 days, no less than five frontal zones passed, producing snow. (See the high wind speeds aloft corresponding to these events in Fig. 6.) This stormy period was followed by a period of more stable weather, similar to the first half of 10 August, mostly with low clouds. A major storm on 11 August lasted a whole day and produced rain at the surface, as evidenced by the "bright band" in the radar reflectivity (Fig. 7b) that coincided with a dramatic increase in the fall velocity of precipitation particles (not shown).

One way to illustrate the impact of the frequent frontal passages on the air masses is through analysis of 5-day back trajectories, here calculated with the McGrath (1989) three-dimensional trajectory model utilizing European Centre for Medium-Range Weather Forecasts (ECMWF) analyses. Trajectories arriving at *Oden*'s position at a height of 800 m, divided into periods with similar characteristics, are shown in Fig. 8. There are long periods with rather similar trajectories separated by very abrupt changes, corresponding to frontal passages. Note, for example, the trajectories for 9–11 August (red lines) from the Greenland Sea, coinciding with the very warmest temperatures aloft in Fig. 4a, abruptly changing to trajectories from the Beaufort Sea (green lines) with the storm on 11 August (Fig. 7). Also, with the exception of shorter periods with air from the Greenland or Kara Seas, note that most trajectories spend at least 5 days over the pack ice before reaching *Oden.*

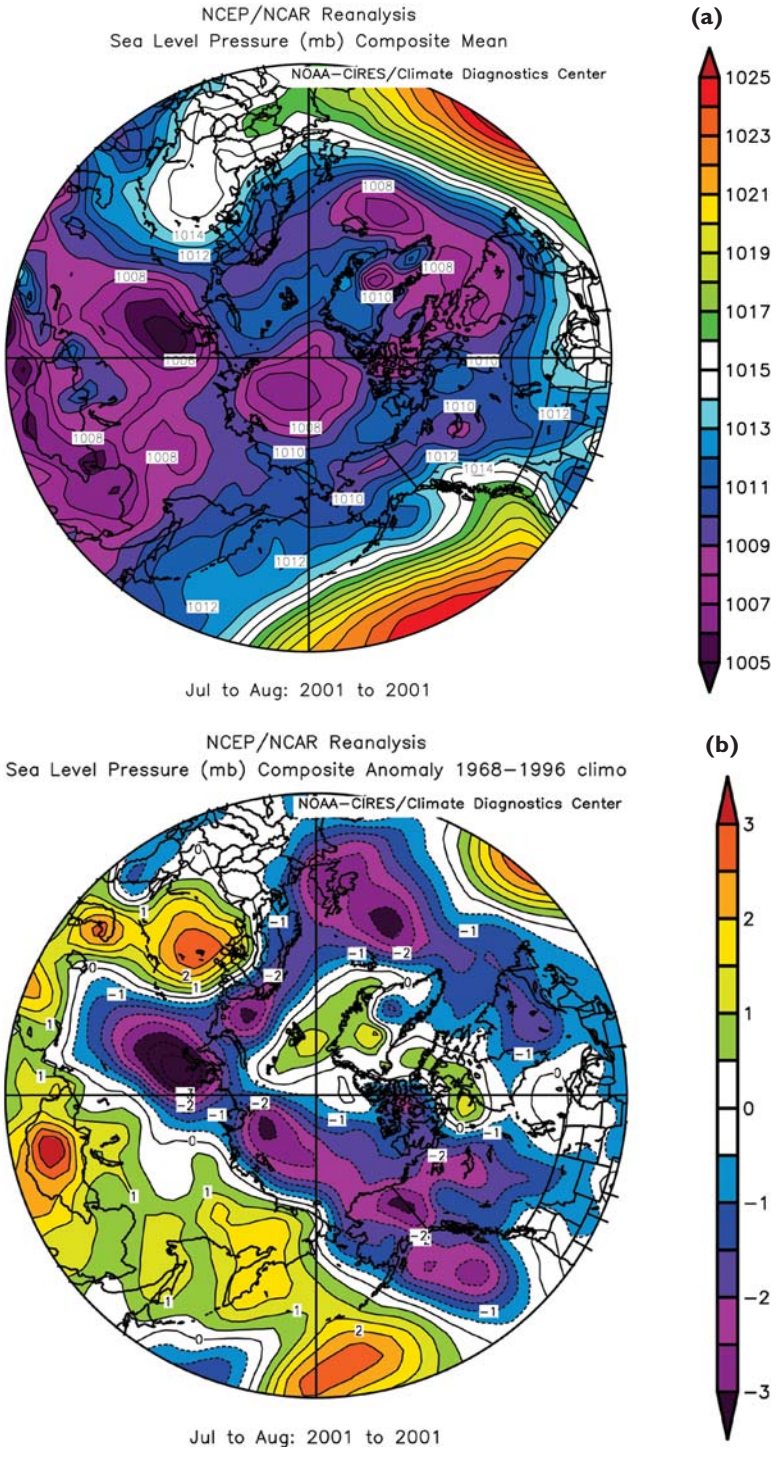


**FIG. 5. Fields of the (a) average and (b) anomalous mean sea level pressure for the months of Jul and Aug 2001 from the NCEP–NCAR reanalysis project. The images were provided by the National Oceanic and Atmospheric Administration (NOAA) Cooperative Institute for Research in Environmental Sciences (CIRES) Climate Diagnostics Center in Boulder, CO (information available online at www.cdc.noaa.gov/).**

**THE INVERSION.** The rawinsoundings were used to derive the vertical structure of the lowest troposphere—the ABL and the capping inversion. Definitions, following

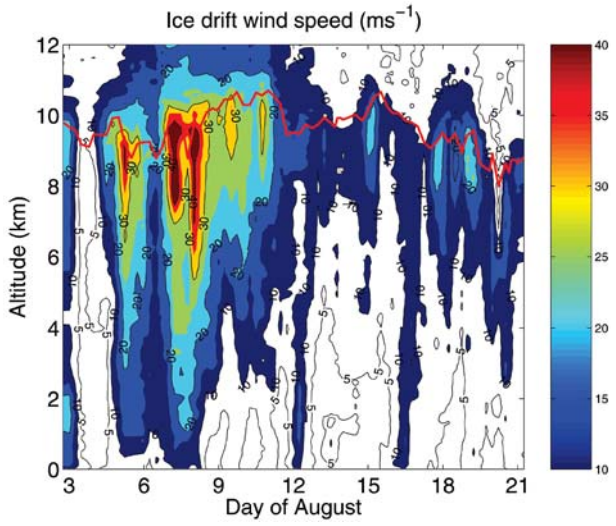


**FIG. 6. Time–height cross section of scalar wind speed (m s$^{-1}$) through the troposphere from the ice-drift period taken from rawinsoundes. Color shading at a 5 m s$^{-1}$ intervals indicates wind speeds > 10 m s$^{-1}$. The thick solid red line shows the tropopause.**

Andreas et al. (2000), are illustrated in Fig. 9. Data from the top and base of the inversion and the surface were extracted from all soundings according to this example. The base of the first main inversion was most often found at ~ 200 m (Fig. 10a). Higher inversion bases were encountered less frequently and strong surface inversions were rare. The inversions were ~ 400 m thick (Fig. 10b) and the temperature differences across the inversion (Fig. 10c) were mostly < 6°C; however, some very strong inversions occurred with temperature differences reaching ~ 18°C.

Figure 11 shows the change in moisture across the inversion. Relative humidity most often remained high across the inversion, indicating that clouds were not always confined by the inversion. Specific humidity often increased across the inversion, in contrast to the typical midlatitude inversion-capped boundary layer, where specific moisture often decreases. In 28% of the soundings this was the case even when relative humidity decreased across the inversion. This seems

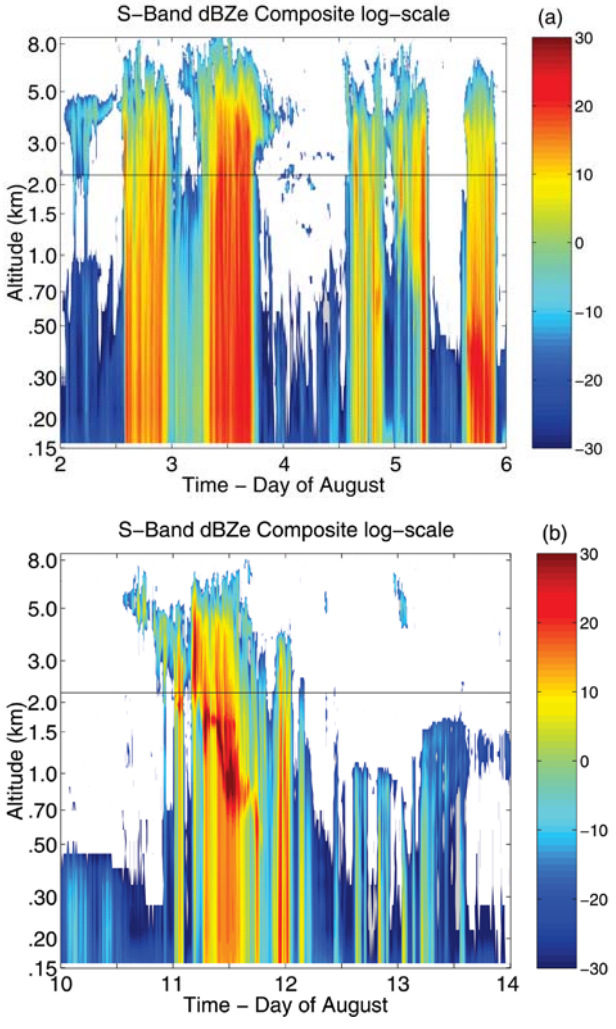


**FIG. 7 (PANELS A AND B AT LEFT). Examples of radar backscatter from the S-band cloud and precipitation radar for two 4-day periods from the ice drift showing several episodes of synoptic-scale frontal systems. The backscatter is proportional to the amount of condensate in clouds or precipitation, with the precipitation/cloud threshold near 0 to +5 dB$Z_e$. Note the logarithmic altitude scale.**

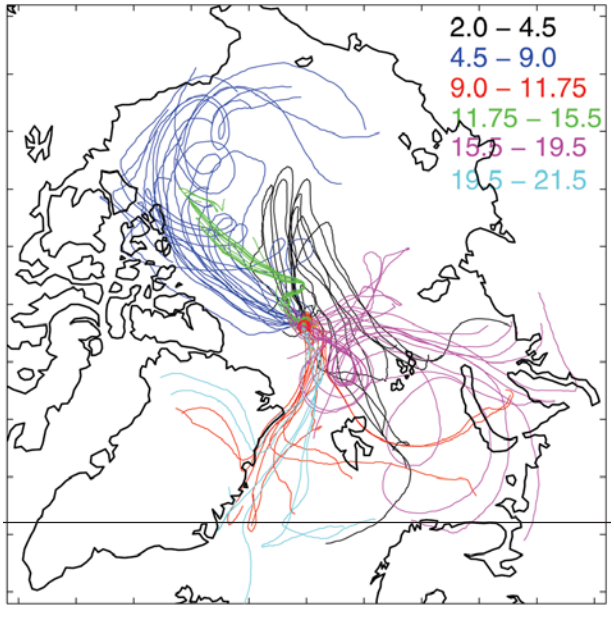


**FIG. 8 (ABOVE). Five-day back trajectories ending at 800 m at the ice-drift camp divided into significant time periods during the ice drift. The periods are given in decimal days of August in the upper right corner of the plot.**

to be a feature specific to the Arctic and implies that entrainment across the inversion will often be a source of boundary layer moisture, rather than a sink, and may, thus, contribute to the maintenance of low-level clouds.

Another feature often quoted to be typical in the ABL is a low-level wind maximum or jet (Nilsson 1996; Andreas et al. 2000). Figure 12 shows normalized low-level wind speed profiles for all cases with a local wind speed maximum near the surface according to the definition in Fig. 9b; ~ 47% of the soundings. The jet typically occurred at a height of 200–400 m, within the inversion, with 5–7 m $s^{-1}$ wind speeds. Using a stricter definition, the number of jets becomes smaller. Only ~ 20% of the profiles remain when a wind speed reduction, from the jet maximum, of 5% and 10% is required to occur at 0.6 and 1.4 times the jet height, respectively. If only cases with a 15% and 30% reduction are retained, just three cases remain.

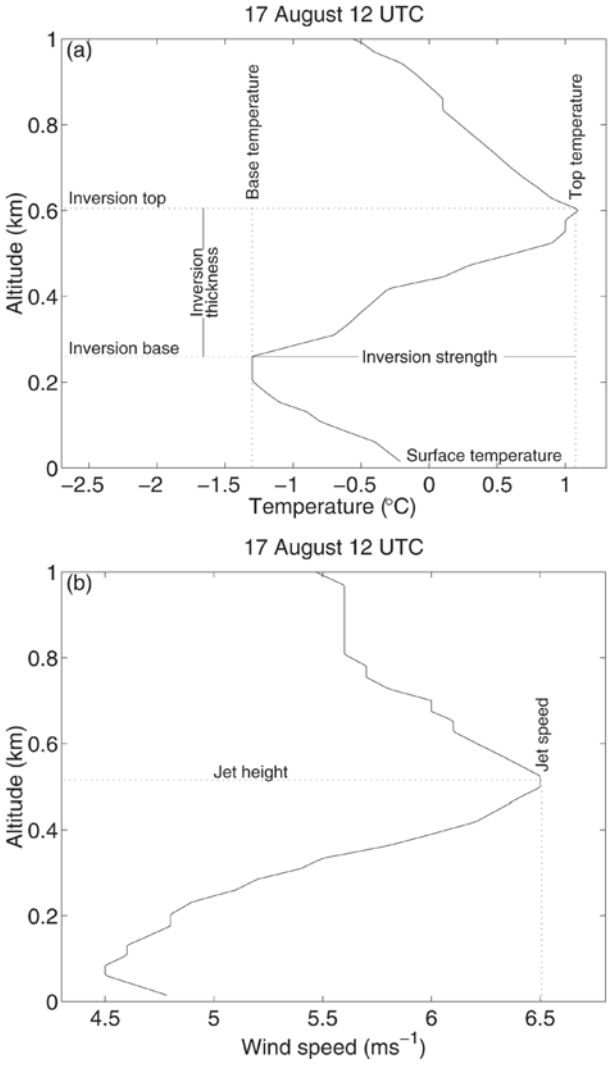


**Fig. 9. Example of rawinsonde profiles of (a) temperature (°C) and (b) wind speed (m $s^{-1}$) taken from 17 Aug 2001. These are provided here as an illustration of some definitions used in the analysis of atmospheric vertical structure.**

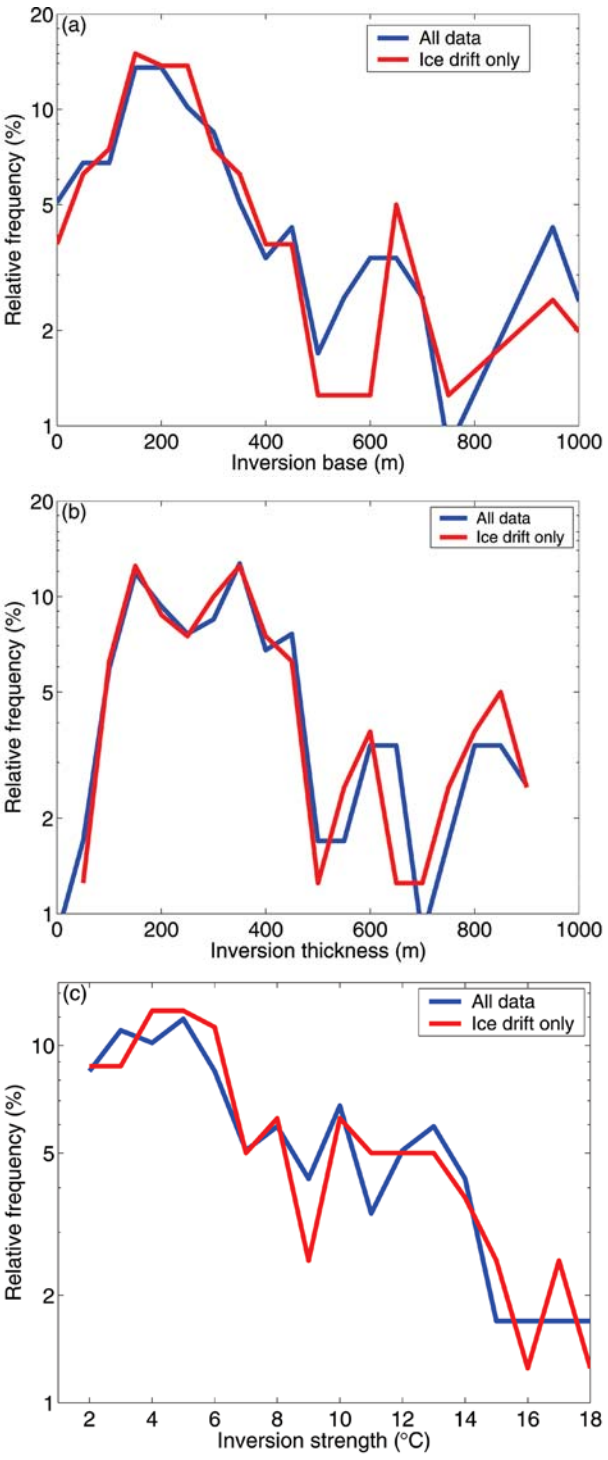


**Fig. 10. Statistics of inversion characteristics based on rawinsonde measurements showing (a) inversion base and (b) inversion thickness (m), (c) inversion strength (°C).**

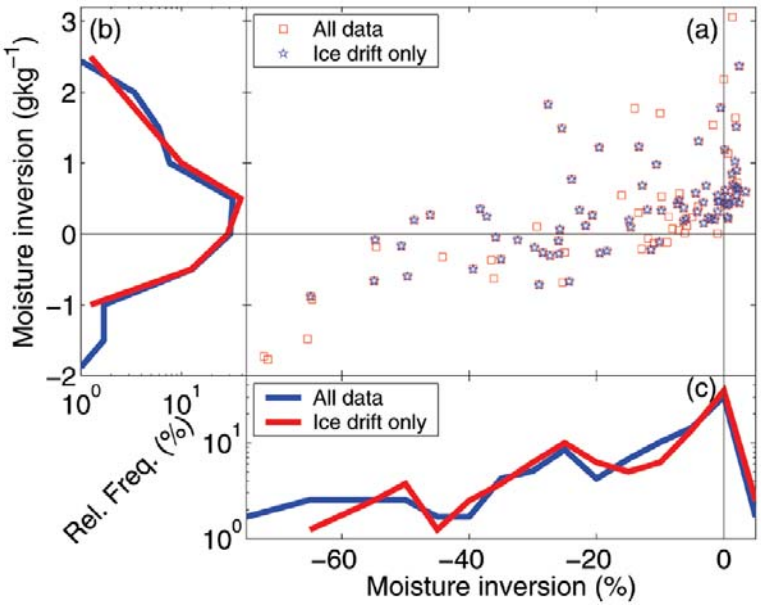


**Fig. 11. The characteristics of the moisture inversion showing (a) a scatterplot of the change in relative and specific humidity over the inversion and statistics of (b) the specific humidity inversion (g kg$^{-1}$) and (c) relative humidity inversion (%). The results are for (blue lines and symbols) the whole experiment and (red lines and symbols) the ice drift only.**

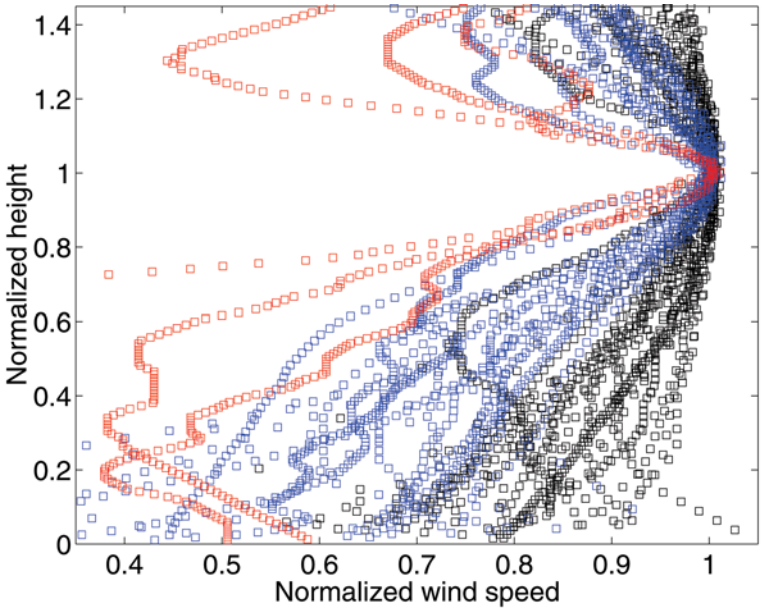


**Fig. 12. Wind speed jet structure showing profiles normalized so that the jet height and the jet wind speed are both unity. Different colors are used for the different criteria: red markers for the stronger criterion, blue markers for the moderate criteria, and black markers for all of the remaining cases. See the text for a discussion.**

With the definition used in Nilsson (1996) and Andreas et al. (2000)—that the wind speed in the jet exceeds the "background" wind speed aloft by at least 2 m s$^{-1}$—about 25% of all cases are retained. The vertical structure was, however, distinctly dissimilar to that described by Nilsson (1996). The jets were weaker with significantly less wind shear below the jet. The wind speed maximum was often embedded in a larger-scale wind shear through a deeper layer, making a determination of a "background" wind aloft difficult. Although it can be expected that wind profiles detected by rawinsoundes are smoother than in reality, these results suggest that conditions may occur in the Arctic that make low-level jets less likely than previously thought.

**THE BOUNDARY LAYER.** The near-surface temperature (Fig. 13a) remained near 0°C for long periods, sometimes dropping to ~ −1° to −2°C. An exception with temperatures down to −6°C appeared during an episode with weak winds and a trajectory from the northwest over the pack ice (see Fig. 8, days of August 11.75–15.5). The statistics of the measurements from the uppermost level in the mast (Fig. 13c) illustrate the strong surface control. Main peaks appear at ~ 0° and ~ −1.7°C, near the melting/freezing points of freshwater and seawater, respectively. When the ambient (advected) air was warmer than ~ 0°C, the melting of snow prevented higher temperatures near the surface. Cooling from brief cold-air episodes also had little effect on the near-surface air, due to the freezing of seawater. The presence of open water (the open ocean between the ice floes or melt ponds on the ice) provided a near-infinite supply of moisture that was mixed into the shallow ABL. Thus, the near-surface relative humidity (Fig. 13b) almost never dropped below 90% and was seldom below 94% (Fig. 13d). The ice, thus, had a very pronounced control over the lower ABL conditions (Andreas et al. 2002).

With this persistently high relative humidity, it is not surprising that the ABL was very cloudy. The

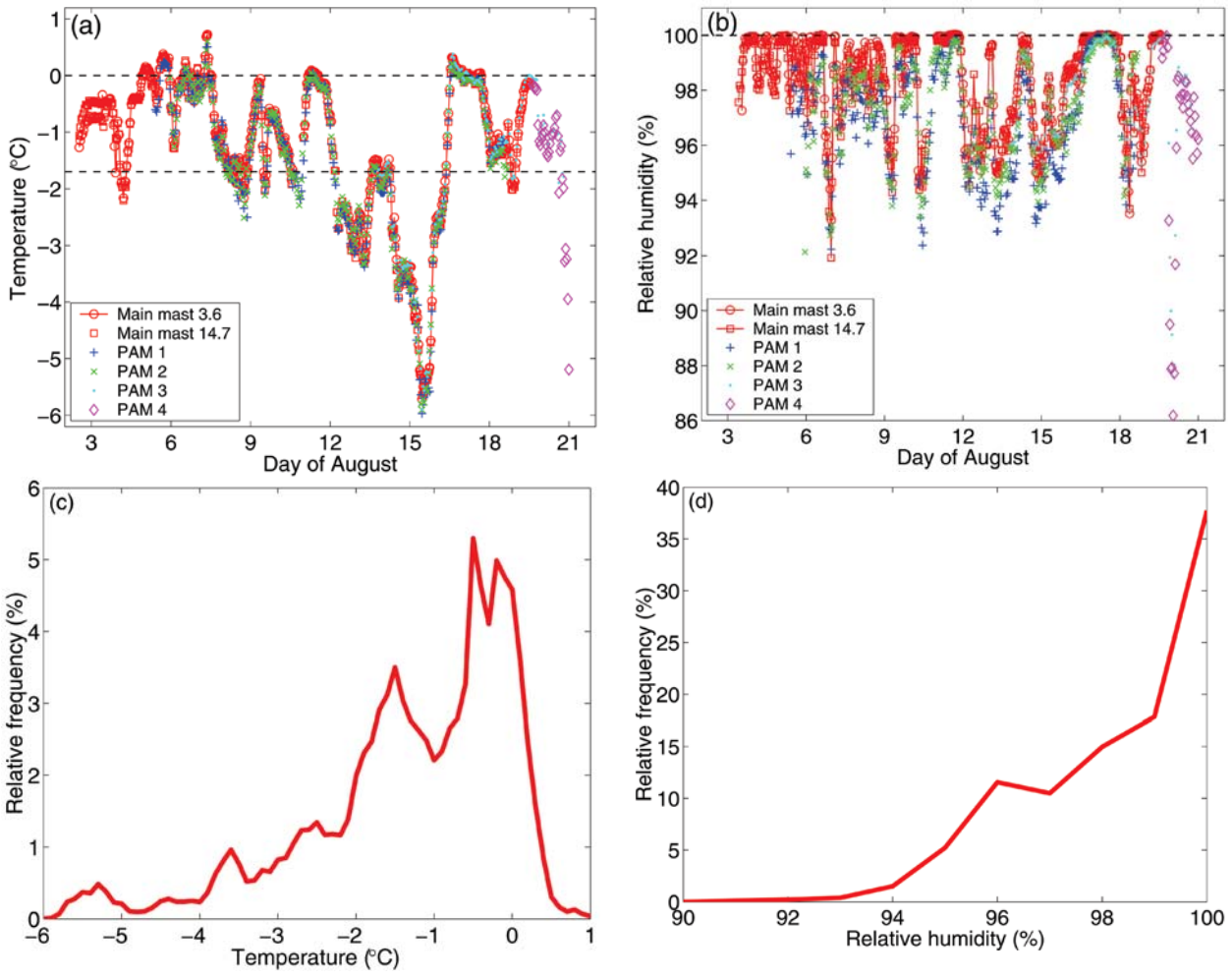


**FIG. 13. Measurements of (a) near-surface temperature (°C) and (b) relative humidity (%) for all the different stations, and statistics of near-surface (c) temperature and (d) relative humidity from the 14.7-m level on the mast. ISFF 1 and 2 were deployed at neighboring ice floes ~ 8 km away from the main site. ISFF 3 was deployed on the main floe, close to the surface of a lead on the opposite edge from the main site. ISFF 4 is a redeployment of one of the main stations close to *Oden* during the tear down of the main site, to maintain measurements as long as possible.**

cloud cover (Fig. 14a) was above 90% for more than half of the total time. Less than 20% cloud cover occurred ~ 20% of the total time and only ~ 10% of the ice drift time. The lowest cloud base was often below ~ 150 m (Fig. 14b). Lower cloud bases were somewhat more common during the ice drift, with a peak around ~ 100 m. These results are consistent with SHEBA observations, where the percentage of cloud occurrence was about 92% and the mean cloud base was about 300 m in August (Intrieri et al. 2002b). No, or only light, precipitation was most common, and was often in the form of drizzle or frozen drizzle. Visibility (Fig. 14c) was either poor (< 1 km) or surprisingly good (> 20 km). Fog (visibility < 1 km) occurred ~ 20% of the total time, somewhat less often during the ice drift. Cases with a cloud base well below 200 m often coincided with a visibility well above 20 km. A particular feature of the summertime Arctic atmosphere, thus, seems to be that the visibility degradation, commonly associated with low cloud bases in midlatitude conditions, is absent. This is likely due to low aerosol particle concentrations, preventing haze formation in the high relative humidity below the low clouds.

The ABL depth was analyzed using a combination of the potential temperature and Richardson Number[3] (Ri) profiles from the soundings. The ABL

[3] Here, $Ri = \frac{g}{\Theta}\frac{\partial \Theta}{\partial z} \Big/ \left(\frac{\partial U}{\partial z}\right)^2$, where $g$ is the gravitational acceleration and $U$ is the scalar wind speed.

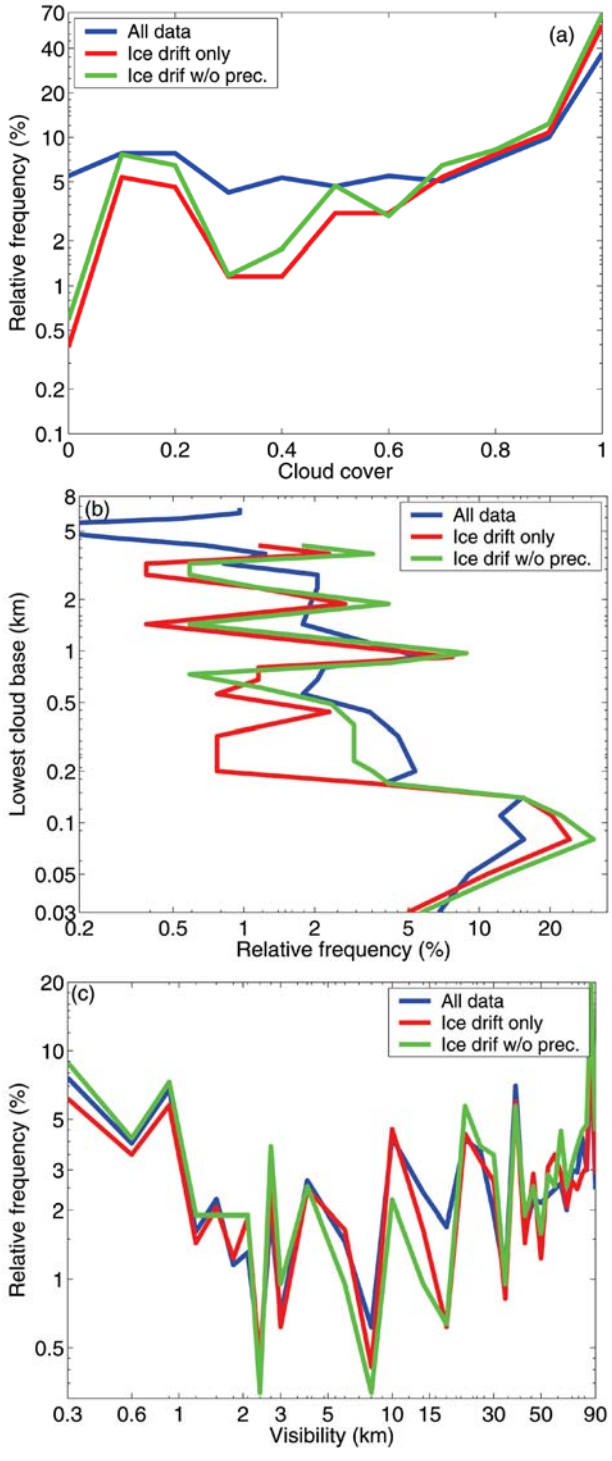


**Fig. 14. Statistics of (a) cloud cover, (b) cloud base (m), and (c) visibility (km) from the whole experiment (blue), the ice drift (red), and the ice drift excluding events with precipitation (green).**

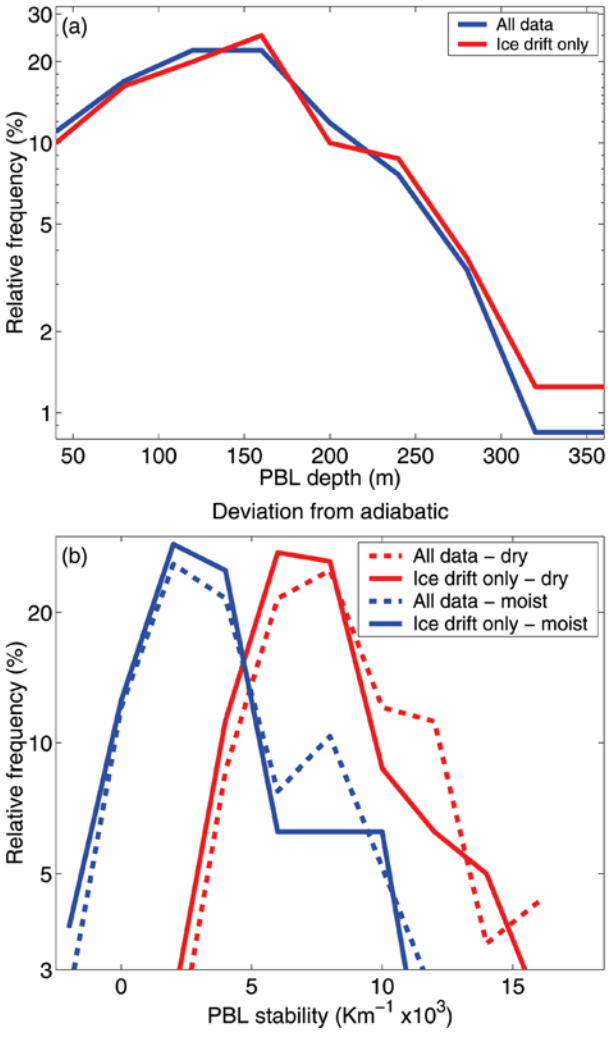


**Fig. 15. Statistics of (a) the depth (m) and (b) the stability $10^{-3}$(K m$^{-1}$) of the boundary layer for the whole experiment (dashed) and the ice drift (solid). The stability is expressed as the deviation from the corresponding dry (red) and moist (blue) adiabatic stability.**

depth was mostly ~ 150 m (Fig. 15a), somewhat lower than the inversion base as defined above. Thus, the lowest clouds often appeared within the ABL. Figure 15b shows the ABL stability, expressed as the deviation of the across-ABL bulk temperature gradient from the corresponding dry and moist adiabatic values. Considering dry adiabatic processes, the ABL was stably stratified; however, with the persistent high relative humidity and the low cloud bases, moist adiabatic processes seem more relevant. In this respect, the ABL appears to have a near-neutral stability. Contrary to some expectations (e.g., Curry 1986), the ABL, thus, remained well mixed. Near-surface well-mixed conditions have been reported previously, both in springtime (Ruffieux et al. 1995; Persson et al. 2002) and late summer (Persson et al. 2002).

Turbulence was measured at two levels on the mast and by the ISFF stations and was highly variable. Figure 16 shows a composite of the turbulence from the highest sonic anemometer (at 15.4 m) and

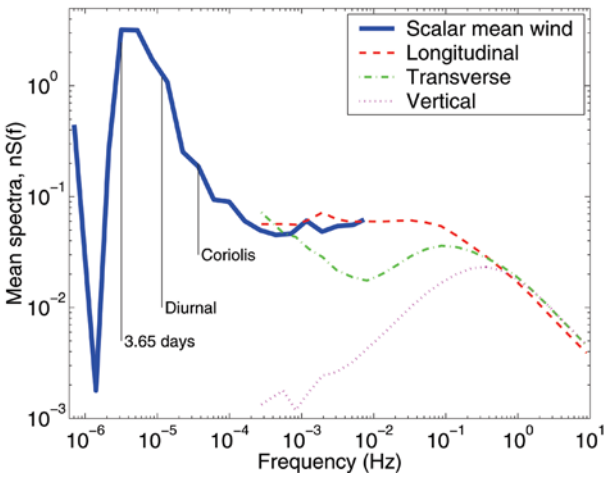


**FIG. 16. Composite plot of power spectra of scalar wind speed (blue) from the topmost cup anemometer in the main mast (at 17.3 m), and the three wind speed components (*U*: red, *V*: green, *W*: cyan) from the topmost sonic anemometer, at 15.4 m. The latter are averages of 257 spectra, calculated over 1-h periods.**

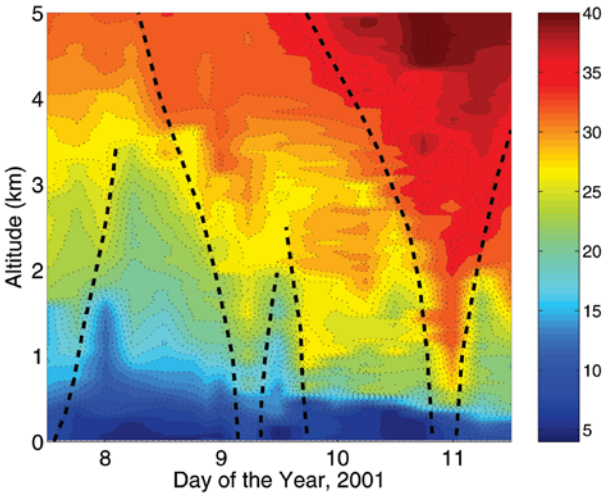


**FIG. 17. Time–height cross section of equivalent potential temperature ($\Theta_e$) for the 8–11 Aug time period, including subjectively analyzed frontal zones (dashed lines). Equivalent potential temperature is conserved during moist adiabatic processes and is often used as an airmass tracer,**

$$\Theta_e = \Theta + \frac{L\Theta}{C_p T} q,$$

**where *L* is the latent heat of vaporization and *q* is the specific humidity, while the temperature *T* is evaluated at the lifting condensation level for unsaturated conditions.**

the 17.3-m cup anemometer. The power spectra of the three wind components are the average of 257 one-hour sonic measurements and are shown to the right, while the corresponding power spectrum of the scalar wind speed from the top cup anemometer is to the left. There is a good match between the power spectra from the sonic and the scalar wind in the overlapping interval. On average, longitudinal spectra do not roll off with decreasing frequency, while the averaged transverse wind speed component shows a pronounced spectral gap. Turbulence spectra have a –2/3 slope at higher frequencies. Minor peaks appear at the diurnal and Coriolis frequencies. The main peak at ~ 3.5 days is consistent with the number of synoptic high-wind events over the 3 weeks. Consistent with the observation that the ABL was mostly near neutral, the buoyancy flux (not shown) was mostly small.

**A CASE STUDY.** In this section, we illustrate the usefulness of this multisensor dataset in examining ABL processes, focusing on a period from the ice drift (8–11 August, Figs. 17–19).

The period started late on 7 August with the passage of a shallow cold front, apparent only below ~ 3–4 km. When the front had passed, the cloud cover gradually broke up and an almost clear 24-h period with good visibility started around 1000 UTC 8 August. The temperature started increasing toward the end of the day, while the wind first weakened but then increased again as the first warm front approached; the warm air behind this system of fronts was already present aloft (> 2–3 km), but the surface warming preceded the front by ~ 12 h. The frontal zone appeared to have a double structure with two warm fronts at the surface, separated by a weak cold front. After the first front passed around 0700 UTC 9 August, the cloud cover increased abruptly and the visibility decreased in a frontal fog. The next warm front passed about half a day later and although the low-level wind direction was mostly from the east (Fig. 18b), the trajectories show that the air above the ABL now came from the Greenland Sea to the south. The second main warm front passed ~ 24 h later, in the evening of 10 August; behind each of the two warm fronts, a pulse of very warm air aloft appeared. Behind the first deep warm front, the air aloft remained dry, while behind the second front relative humidity aloft also increased (see Fig. 4). After the second warm front, the temperature at 0.8 km peaked at ~ 8°C at midnight between 10 and 11 August; the 9–11 August period had the strongest inversion observed during the ice drift. Note that although the air aloft was dramatically warmed, the ABL temperature decreased from about midday on 9 August and did not increase again until after the cold front.

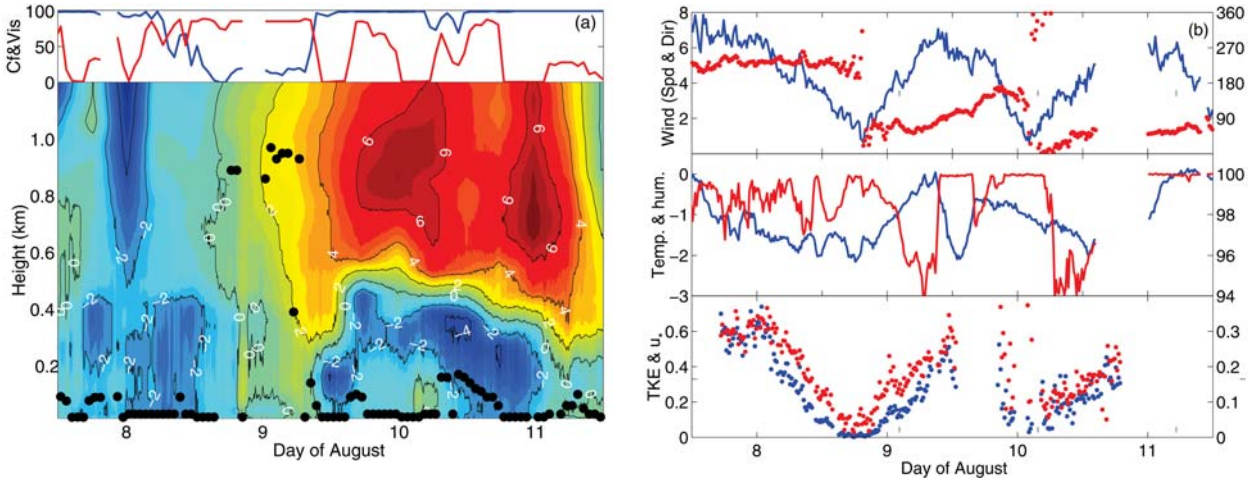


**FIG. 18. A summary figure from multiple-sensor measurement time series for the same period as that of Fig. 17. The plots show (a) time–height cross sections of temperature (°C) from the scanning radiometer, with (●) 1-h-averaged cloud base inserted, and cloud fraction (%; blue) and visibility (km; red) on top, also from 1-h averages. (b) A summary of measurements from the mast (from the top down): wind speed (m $s^{-1}$; blue), wind direction (°; red), temperature (°C; blue), relative humidity (%; red), turbulent kinetic energy ($m^2$ $s^{-2}$; blue), and friction velocity (m $s^{-1}$; blue). Note the different scales on the left and right of each panel, corresponding to the blue and red data points, respectively.**

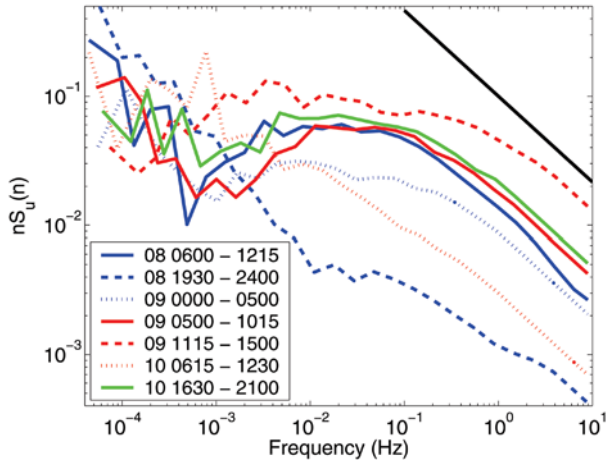


**FIG. 19. Power spectra of the along-wind component for all the long periods (~ 6 h) available during the episode in Figs. 17–18, as given by the legend (DD-TTTT–TTTT).**

Note the arrival of the first warm front, seen very clearly in the radiometer cross section (Fig. 18a). It appears that vertical mixing from the free troposphere down into the ABL was facilitated by the frontal passage. The period ended with the arrival of a cold front shortly after the last main warm front passed, a few hours into 11 August. This frontal passage can also be seen in the radiometer record, although its signal is weaker. The temperature, however, started increasing and it appears that other processes, presumably the radiation–cloud interaction and turbulent mixing, controlled the ABL temperature. Thus, warm fronts do not necessarily signify ABL warming, nor do cold fronts necessarily indicate ABL cooling. While the level of turbulence varied widely during the period, the most pronounced feature in the power spectra (Fig. 19) is a spectral gap, at about a half-hour period, with almost unchanged mesoscale variability in the wind speed at even lower frequencies.

This example illustrates the strength of analyzing multisensor in situ and remote sensing measurements simultaneously. In particular, the scanning radiometer resolves details on important events in the lower troposphere. Shallow, presumably mesoscale, frontal zones, as revealed by the $\Theta_e$ analysis or the radiometer temperatures, were more frequent than the more obvious synoptic-scale fronts, which brought deep clouds and precipitation. Many of the former were shallow, and the associated ABL air often seemed to have a different origin than the air aloft. Consequently, near-surface measurements are poor indicators of frontal activity, and only the combination of many sensors reveals details of the mesoscale structure of these events. The scanning radiometer reveals interesting episodes of apparently strong entrainment tied to frontal passages. This suggests that mixing of free-troposphere air into the ABL may occur in intense, but short and infrequent bursts linked to frontal passages.

**CONCLUSIONS.** Much more careful analysis will be required before the main objectives, listed at the

beginning of this paper, are met. Some tentative conclusions are the following:

- Synoptic-scale activity with deeper cloud systems and precipitation occurred relatively frequently, but shallow mesoscale frontal zones appeared even more often. Back trajectories indicate that boundary layer air often had a different origin than air only a few hundred meters above the boundary layer. While the latter changed origin abruptly with major synoptic events, the former seemed much more variable. This indicates that the formation of shallow mesoscale systems is an important feature for the Arctic boundary layer.
- Very strong capping inversions sometimes occurred, with the highest temperatures well above 0°C around ~ 1 km. In contrast to the midlatitude cloud-capped boundary layer, specific moisture often increased with height over the capping inversion. These features are believed to be consequences of advection of warm and moist air from surrounding open oceans. As this air enters the pack ice, it cools at the surface to ~ –2° to 0°C. Local mixing maintains a shallow near-mixed cool and moist layer, and a strong inversion at the interface to the free troposphere.
- The summer boundary layer was very moist and cloudy but well mixed, and surface inversions seldom appeared. Vertical mixing between the boundary layer and the free troposphere appeared to be related to the passage of frontal zones. Low-level wind speed maxima (low-level jets) were weak, and strong jets occurred rarely.
- Low-level clouds dominated with the most common cloud base around 100 m. Very low cloud bases (< 100 m) often coincided with surprisingly good visibility (> 20 km), probably because very low concentrations of aerosols prevented the formation of haze.
- Near-surface temperature remained mostly between –1.5° and 0°C, controlled by the melting/freezing of either snow at the surface of the ice or the salty ocean water. Relative humidity seldom dropped below 94%, even when the low clouds dissipated.

While AOE-2001 was a major undertaking, requiring several years of planning, its most intensive measurement phase during the ice drift lasted only 3 weeks. Although our instrumentation setup allowed fairly detailed analysis of the boundary layer structure, the sampling time was too limited to apply any kind of climatic perspective. Some of our observations are at odds with previous statements about the central Arctic boundary layer. This illustrates the need for more experimental boundary layer campaigns to the central Arctic, rather than indicating that the current or previous observations may have been in error. The interannual and spatial variability of the boundary layer structure in the Arctic is simply not understood well enough for any short-term experiment to claim climatic representativity.

On the other hand, this experiment utilized instrumentation with temporal and spatial resolution not previously used over the Arctic pack ice and was located far north in a less explored sector of the Arctic basin. Hence, the results complement earlier experiments and broaden the climatic perspective. We believe that findings from process-oriented studies based on this dataset can be invaluable for developing our understanding of the Arctic boundary layer and for improving the models that are used for simulating Arctic climate.

**ACKNOWLEDGMENTS.** This research was made possible by grants from the Swedish Natural Science Research Council (NFR), the Knut and Alice Wallenberg Foundation, and the Swedish Secretariat for Polar Research (Polar). The icebreaker *Oden* and logistics for the expedition were provided by Polar. The dedicated work by Scott Abbott and John Militzer before and during the expedition was essential to the results. We also acknowledge the work by Leif Bäcklin and Nils Wahlberg, without which many of the measurements would never have been taken. Allen White, Vladimir Leuskiy, and Brian Templeman performed the processing of the remote sensing data. Special thanks go to Bertil Larsson and Eric Erixon for help with the weather station and rawinsoundings on board *Oden,* as well as many other things. We also express special thanks to all other participants in the AOE-2001 expedition, for unselfish help with the numerous problems bound to appear in a field program far away into the Arctic ice. Finally, sincere thanks to all of the crew on *Oden* and to the logistics staff from Polar; your assistance with many practical matters was invaluable.

## REFERENCES

Andreas, E., K. J. Klaffey, and A. P. Makshtas, 2000: Low level atmospheric jets and inversions over the Western Weddell Sea. *Bound.-Layer Meteor.,* **97,** 459–486.

——, P. S. Guest, P. O. G. Persson, C. W. Fairall, T. W. Horst, R. E. Moritz, and S. R. Semmer, 2002: Near-surface water vapor over polar sea ice is always near ice-saturation. *J. Geophys. Res.,* **107,** 8033, doi:10.1029/2000JC000411.

Battisti, C. M., C. M. Bitz, and R.M. Moritz, 1997: Do general circulation models underestimate the natural variability in the Arctic climate? *J. Climate,* **10,** 1909–1920.

Beesley, J. A., C. S. Bretherton, C. Jacob, E. L Andreas, J. M. Intrieri, and T. A. Uttal, 2000: A comparison of cloud and boundary layer variables in the ECMWF forecast model with observations at the Surface Heat and Energy of the Arctic (SHEBA) ice camp. *J. Geophys. Res.,* **105** (D10), 12 337–12 349.

Bigg, E. K., and C. Leck, 2001: Cloud-active particles over the central Arctic area. *J. Geophys. Res.,* **106** (D23), 32 155–32 166.

——, ——, and E. D. Nilsson, 1996: Sudden changes in Arctic atmospheric aerosol concentrations during summer and autumn. *Tellus,* **48,** 254–271.

——, ——, and E. D. Nilsson, 2001: Sudden changes in aerosol and gas concentration in the central Arctic marine boundary layer: Causes and consequences. *J. Geophys. Res.,* **106** (D23), 32 167–32 185.

Chapman, W. L., and J. E. Walsh, 1993: Recent variations of sea ice and air temperature in high latitudes. *Bull. Amer. Meteor. Soc.,* **74,** 33–47.

Comiso, J. C., 2002: A rapidly declining perennial sea ice cover in the Arctic. *Geophys. Res. Lett.,* **29**, 1956, doi:10.1029/2002GL015650.

Curry, J. A., 1986: Interactions among turbulence, radiation and microphysics in Arctic stratus clouds. *J. Atmos. Sci.,* **43,** 90–106.

——, and Coauthors, 2000: FIRE Arctic clouds experiment. *Bull. Amer. Meteor. Soc.,* **81,** 5–29.

Grachev, A. A., C. W. Fairall, P. O. G. Persson, E. L Andreas, and P. S. Guest, 2004: Stable boundary-layer scaling regimes: The SHEBA data. *Bound.-Layer Meteor.,* in press.

Houghton, J. T., Y. Ding, D. J. Griggs, M. Nogner, P. J. van der Linden, X. Dai, K. Maskell, and C. C. Johnson, Eds., 2001: *Climate Change 2001: The Scientific Basis.* IPCC Rep., 881 pp.

Intrieri, J. M., C. W. Fairall, M. D. Shupe, P. O. G. Persson, E. L Andreas, P. S. Guest, and R. E. Moritz, 2002a: An annual cycle of Arctic surface cloud forcing at SHEBA. J. *Geophys. Res.,* **107,** 8039, doi:10.1029/2000JC000439.

——, M. D. Shupe, T. Uttal, and B. J. McCarty, 2002b: An annual cycle of Arctic clouds characteristics observed by radar and lidar at SHEBA. *J. Geophys. Res.,* **107,** 8030, doi:10.1029/2000JC000423.

Kahl, J. D., N. A. Zaitseva, V. Khattatov, R. C. Schnell, D. M. Bacon, J. Bacon, V. Radionov, and M. C. Serreze, 1999: Radiosonde observations from the former Soviet "North Pole" series of drifting ice stations, 1954–90. *Bull. Amer. Meteor. Soc.,* **80,** 2019–2026.

Kalnay, E., and Coauthors, 1996: The NCEP/NCAR 40-Year Reanalysis Project. *Bull. Amer. Meteor. Soc.,* **77,** 437–471.

Leck, C., and C. Persson, 1996: Seasonal and short-term variability in dimethyl sulfide, sulfur dioxide and biogenic sulfur and sea salt aerosol particles in the arctic marine boundary layer, during summer and autumn. *Tellus,* **48B,** 272–299.

——, and E. K. Bigg, 1999: Aerosol production over remote marine areas—A new route. *Geophys. Res. Lett.,* **26,** 3577–3580.

——, ——, D. S. Covert, J. Heintzenberg, W. Maenhaut, E. D. Nilsson, and A. Wiedensohler, 1996: Overview of the atmospheric research program during the International Ocean Expedition of 1991 (IAOE-1991) and its scientific results. *Tellus,* **48B**, 136–155.

——, E. D. Nilsson, E. K. Bigg, and L. Bäcklin, 2001a: The atmospheric program of the Arctic Ocean Expedition 1996 (AOE-1996)—An overview of scientific objectives, experimental approaches and instruments. *J. Geophys. Res.,* **106** (D23), 32 051–32 067.

——, M. Norman, E. K. Bigg, and R. Hillamo, 2001b: Chemical composition and sources of the high Arctic aerosol relevant for cloud formation. *J. Geophys. Res.,* **107** (D12), 1–17, doi:10.1029/2001JD001463.

——, M. Tjernström, P. Matrai, E. Swietlicki, and E. K. Bigg, 2004: Can marine microorganisms influence melting of the Arctic pack ice. *Eos, Trans. Amer. Geophys. Union,* **85,** 25–36.

Mahrt, L., 1998: Stratified atmospheric boundary layers and breakdown of models. *Theor. Comput. Fluid Dyn.,* **11,** 263–279.

McGrath, 1989: Trajectory models and their use in the Irish Meteorological Service. Irish Meteorological Service, Tech. Memo. 112/89, 12 pp.

Meehl, G. A., G. J. Boer, C. Covey, M. Latif, and R. J. Stouffer, 2000: The Coupled Model Intercomparison Project (CMIP). *Bull. Amer. Meteor. Soc.,* **81,** 313–318.

Morison, J. H., K. Aagaard, and M. Steele, 2000: Recent environmental changes in the Arctic: A review. *Arctic,* **53,** 4.

Nilsson, E. D., 1996: Planetary boundary layer structure and air mass transport during the International Arctic Ocean Expedition 1991. *Tellus,* **48B,** 178–196.

Parkinson, C., D. J. Cavalieri, P. Gloersen, H. J. Zwally, and J. C. Comiso, 1999: Arctic sea ice extents, areas, and trends, 1978–1996. *J. Geophys. Res.,* **104,** 20 837–20 856.

Perovich, D. K., and Coauthors, 1999: Year on ice gives climate insights. *Eos, Trans. Amer. Geophys. Union,* **80,** 483–486.

Persson, P. O. G., C. W. Fairall, E. L Andreas, P. S. Guest, and D. K. Perovich, 2002: Measurements near the At-

mospheric Surface Flux Group tower at SHEBA: Near-surface conditions and surface energy budget. *J. Geophys. Res.,* **107,** 8045, doi:10.1029/2000JC000705.

Persson, P. O. G., E. L Andreas, C. W. Fairall, P. S. Guest, and D. K. Perovich, 2003: Pack ice surface energy changes at SHEBA initiated by late summer synoptic forcing. Preprints, *Seventh Conf. on Polar Meteorology and Oceanography and Joint Symp. on High-Latitude Climate Variations*, Hyannis, MA, Amer. Meteor. Soc., CD-ROM 3.21.

Räisänen, J., 2001: $CO_2$-induced climate change in the Arctic area in the CMIP2 experiments. *SWECLIM Newsletter,* Vol. 11, 23–28. [Available from Swedish Meteorological and Hydrological Institute, SE-601 76 Norrköping, Sweden.]

Rigor, I. G., R. L. Colony, and S. Martin, 2000: Variations in surface air temperature observations in the Arctic, 1979–97. *J. Climate,* **13,** 896–914.

Ruffieux, D. R., P. O. G. Persson, C. W. Fairall, and Dan E. Wolfe, 1995: Ice pack and lead surface energy budgets during LEADEX 92. *J. Geophys. Res.,* **100** (C3), 4593–4612.

Serreze, M. C., and Coauthors, 2000: Observational evidence of recent change in the northern high-latitude environment. *Climate Change,* **46,** 159–207.

Thompson, D. W. J., and J. M. Wallace, 1998: The Arctic Oscillation signature in the wintertime geopotential height and temperature fields. *Geophys. Res. Lett.,* **25,** 1297–1300.

Tjernström, M., C. Leck, P. O. G. Persson, M. L. Jensen, S. P. Oncley, and A. Targino, 2004: Experimental equipment. *Bull. Amer. Meteor. Soc.,* **85,** doi:10.1175-BAMS-85-9-Tjernstrom.

Uttal, T., and Coauthors, 2002: Surface Heat Budget of the Arctic Ocean. *Bull. Amer. Meteor. Soc.,* **83,** 255–276.

Walsh, J. E., W. M. Kattsov, W. L. Chapman, V. Govorkova, and T. Pavlova, 2002: Comparison of Arctic climate by uncoupled and coupled global models. *J. Climate,* **15,** 1429–1446.